

Numerical studies of Ising spin glasses in two, three, and four dimensions

R. N. Bhatt

AT&T Bell Laboratories, Murray Hill, New Jersey 07974-2070

A. P. Young

Department of Physics, University of California, Santa Cruz, California 95064

(Received 24 July 1987)

We present the results of numerical simulations on Ising spin glasses in zero magnetic field with nearest-neighbor interactions on hyper-cubic lattices in two, three, and four dimensions with both Gaussian and $\pm J$ bond distributions. Finite-size scaling is used to analyze the results. In two dimensions ($d=2$) we agree with earlier work that the transition temperature is at $T_c=0$, and obtain the correlation-length exponent ν , and the exponent η , at the zero-temperature transition for the $\pm J$ model. In $d=3$ dimensions we concentrate on results for the Gaussian distribution, since our results for the $\pm J$ distribution have been presented earlier. As expected, we find similar results for the two distributions, namely a nonzero T_c but evidence that $d=3$ is close to the lower critical dimension. In a four-dimensional spin glass with Gaussian bonds we find that *only a modest amount* of computer time is required to show that T_c is nonzero with a long-range-ordered phase below T_c . Our estimates for critical exponents in $d=4$ dimensions agree well with results from recent high-temperature-series expansions.

I. INTRODUCTION

Spin glasses present a great challenge for numerical simulations. The effects of frustration and disorder lead to slow dynamics, with a roughly logarithmic time dependence, so simulations must be run for many time steps. Furthermore, quenched in disorder gives rise to large sample to sample fluctuations making an average over many samples necessary to obtain accurate results. Nonetheless, simulations have played an important role¹ in understanding basic issues in spin glasses (such as the existence of a phase transition in short-range models and the lower critical dimension). This has been possible because of special purpose computers,^{2,3} high-speed general-purpose machines such as the Distributed Array Processor at Queen Mary College, London,^{4,5} and techniques such as finite-size scaling⁶ which allows one to squeeze the maximum information from data on small systems. In fact, we shall see that using a finite-size-scaling analysis on data obtained with *only modest computer power* one can obtain interesting results, such as $d=4$ being *above* the lower critical dimensions, d_l (rather than $d_l=4$ which was widely accepted for a long time).

In this paper we present the results of our simulations on Ising spin glasses with short range interactions in dimension $d=2, 3$, and 4 in the absence of a magnetic field. We have studied both a Gaussian distribution of bonds and a binary or $\pm J$ distribution to check the expected universality of behavior when the transition temperature T_c is nonzero. Indeed, the critical exponents which we estimate from our results presented here for the Gaussian distribution in $d=3$ are consistent with those obtained previously³ for the binary distribution, and our four-dimensional results with a Gaussian distribution agree with a recent high-temperature-series analysis⁷ for $\pm J$

bonds. The transition in $d=2$ is at $T_c=0$, where the $\pm J$ distribution gives different results from a continuous distribution because it has a large ground-state degeneracy with finite entropy. Our finite size scaling approach gives results in agreement with previous large scale work for the two exponents, η and ν , which describe this transition.

Our earlier work⁵ on the three dimensional $\pm J$ model did not clearly show whether or not the spin-glass order parameter was finite below T_c . Despite inclusion of larger sizes and lower temperatures in the finite-size-scaling analysis from subsequent runs by A. T. Ogielski, this question has remained unanswered. However, in $d=4$ dimensions a similar analysis clearly shows ordering. A possible explanation is that ordering also occurs in three dimensions but that corrections to finite size scaling, which are important close to d_l mask the effect for the small lattice sizes studied. Similar effects are also seen in power-law one-dimensional (1D) models⁸ as the power is increased and the model becomes short range with no transition.

The plan of this paper is as follows. Section II describes the model used and discusses the relevant quantities that we have chosen to calculate. A good deal of thought has gone into ensuring that our simulations are run for long enough to be in equilibrium. We discuss in some detail our techniques for doing this in Sec. III. Our results and analysis for $d=2, 3$, and 4 are given in Secs. IV–VI respectively, and our conclusions are summarized in Sec. VII.

II. THE MODEL

The standard model of a spin glass⁹ is described by the Hamiltonian

$$H = - \sum_{\langle ij \rangle} J_{ij} S_i S_j \quad (1)$$

where the exchange interaction J_{ij} between the spins S_i are treated as quenched random variables. In general S_i can be n -component vectors; however we consider only the Ising case, where $S_i = \pm 1$. Further, we restrict ourselves to distributions of interactions which have no net ferromagnetic or antiferromagnetic tendencies. For this *pure* spin glass case the J_{ij} are equally negative and positive; consequently $[J_{ij}]_{av} = 0$ where $[\dots]_{av}$ indicates an average over the bond distribution. Following Edwards and Anderson,⁹ realistic spin glasses [randomly positioned localized moments in metals interacting with an oscillatory Ruderman-Kittel-Kasuya-Yosida (RKKY) interaction $\propto r_{ij}^{-3}$, or site diluted spins in systems where the interaction is short range], are often modeled by spins on a lattice with short range (usually nearest neighbor) interaction described by a specified probability distribution $P(J_{ij})$. Two distributions have been used most commonly:

$$P(J_{ij}) = \frac{1}{2} [\delta J_{ij} - J] + \delta(J_{ij} + J) \quad (2a)$$

known as the $\pm J$ distribution, and

$$P(J_{ij}) = \frac{1}{\sqrt{2\pi J^2}} e^{-J_{ij}^2/2J^2} \quad (2b)$$

or the Gaussian distribution. In both cases the energy scale is chosen such that $[J_{ij}^2]_{av} = 1$. In mean field theory the transition is at $T_c^{MF} = z^{1/2}$, where z is the coordination number of the lattice. We will consider d -dimensional simple hypercubic lattices with nearest neighbor interactions (only), so $z = 2d$, with the above two distributions.

The spin-glass (SG) transition for zero magnetic field is characterized by a divergence of the spin-glass susceptibility when approached from the high-temperature (paramagnetic) phase:

$$\chi_{SG} = \frac{1}{N} \left[\sum_{ij} \langle S_i S_j \rangle_T^2 \right]_{av}, \quad (3)$$

where the $\langle \dots \rangle_T$ denotes a thermal (time) average for a given realization of bonds J_{ij} and $[\dots]_{av}$ a bond average. $N = L^d$ is the number of spins. In the paramagnetic phase, χ_{SG} is related to the nonlinear susceptibility (the coefficient of the h^3 term in the expansion of magnetization $M \equiv \langle \sum_i S_i \rangle_T$ in powers of the applied field, h). In an infinite system

$$\chi_{SG} \sim (T - T_c)^{-\gamma}, \quad (4)$$

with

$$\gamma = (2 - \eta)\nu, \quad (5)$$

where ν is the exponent of the spin glass correlation length ξ for $T \gtrsim T_c$, and η describes the power law decay of the correlation at T_c . Thus:

$$G_2(r_{ij}) \equiv [\langle S_i S_j \rangle_T^2]_{av} \sim \frac{f(r_{ij}/\xi)}{r_{ij}^{d-2+\eta}} \quad (T \gtrsim T_c). \quad (6)$$

where ξ diverges as

$$\xi \sim (T - T_c)^{-\nu}. \quad (7)$$

For $r \gg \xi$, $f(r/\xi) \sim \exp(-r/\xi)$.

The Edwards-Anderson spin-glass order parameter below T_c is given by

$$q = [\langle S_i \rangle_T^2]_{av} \sim (T_c - T)^\beta \quad (8)$$

and, by hyperscaling,

$$\beta = \frac{\nu}{2} (d - 2 + \eta) \quad (9)$$

where d is the physical dimension of the system.

Thus, for a nonzero T_c , there are two independent static exponents in spin glasses, just as in uniform systems. Below the lower critical dimension d_l , the low-temperature behavior is governed by a zero-temperature critical point, as if the system had a transition at zero temperature ($T_c = 0$). In this case, there is an additional relation¹⁰ between the exponents *provided the ground state is nondegenerate* (aside from symmetry related states):

$$2 - \eta = d \quad (T_c = 0) \quad (10)$$

so that

$$\gamma = d\nu \quad (T_c = 0). \quad (11)$$

Consequently, there is only one independent static exponent if $T_c = 0$. This is *not* true for the $\pm J$ model where the ground state is extensively degenerate.

In Monte Carlo simulations, it is convenient to replace thermal averages by time averages, and a natural quantity to study is the spin auto correlation function

$$q(t) = \frac{1}{N} \left[\sum_i S_i(t_0) S_i(t_0 + t) \right]_{av} \quad (12)$$

where the initial time t_0 is an equilibration time (see Sec. III). Note that t in Eq. (3), and all subsequent equations, is the time measured *after* the equilibration time t_0 . For any finite system in zero external field, $q(t) \rightarrow 0$ as $t \rightarrow \infty$, because of flips of the entire lattice. Unlike the ferromagnet, however, for spin glasses there does not appear to be a simple method for clear separation of the ensemble averaged time scales for equilibrium within one free energy minimum and between minima (including lattice flips).

Another relevant quantity is the time-dependent four-spin-correlation function:

$$\chi_{SG}(t) = \frac{1}{N} \left[\left[\sum_i S_i(t_0) S_i(t_0 + t) \right]^2 \right]_{av} \quad (13)$$

which is easily shown to converge to the spin glass susceptibility χ_{SG} [Eq. (3)] in the $t \rightarrow \infty$ limit.

In fact, $q(t)$ and $\chi_{SG}(t)$ are just the first two moments of the distribution of the overlap

$$Q(t) = \frac{1}{N} \sum_i S_i(t_0) S_i(t_0 + t) \quad (14)$$

($-1 \leq Q(t) \leq 1$) and it is useful to study the probability distribution of $Q(t)$ in the $t \rightarrow \infty$ limit. In practice we compute this distribution for times larger than t_0 *after* the initial equilibration; thus

$$P(q) = \frac{1}{\tau_0 - t_0 + 1} \left[\sum_{t=t_0}^{\tau_0} \delta[q - Q(t)] \right]_{\text{av}}, \quad (15)$$

where τ_0 ($\geq t_0$) is the number of steps which are simulated after the equilibration time t_0 , and the sum starts at $t = t_0$ as discussed in Sec. III. It is also useful, as we shall see in Sec. III, to calculate $P(q)$ from two identical copies of the system, $\{S_i^1(t)\}$ and $\{S_i^2(t)\}$, with the *same* realization of bonds J_{ij} , running independently in parallel. Then the instantaneous mutual overlap

$$Q'(t) = \frac{1}{N} \sum_i S_i^1(t_0 + t) S_i^2(t_0 + t) \quad (16)$$

has the same distribution as $Q(t)$ in the $t \rightarrow \infty$ limit (since the second system may be considered as a realization of the first after a long time) so $P(q)$ is also given by

$$P(q) \equiv \frac{1}{\tau_0} \left[\sum_{t=1}^{\tau_0} \delta\{q - Q'(t)\} \right]_{\text{av}}. \quad (17)$$

Clearly, χ_{SG} may be obtained as the second moment of $P(q)$:

$$\chi_{\text{SG}} = N \int_{-1}^1 q^2 P(q) dq \quad (18a)$$

$$= \frac{1}{N\tau_0} \left[\sum_{t=1}^{\tau_0} \left[\sum_i S_i^1(t_0 + t) S_i^2(t_0 + t) \right]^2 \right]_{\text{av}}. \quad (18b)$$

It is particularly interesting to look at the dimensionless parameter

$$g_L = \frac{1}{2} \left[3 - \frac{\langle q^4 \rangle}{\langle q^2 \rangle^2} \right] \quad (19)$$

where $\langle \dots \rangle \equiv \int (\dots) P_L(q) dq$ where $P_L(q)$ is the overlap distribution, defined by Eq. (17) for a system of linear dimension L . In the paramagnetic phase for $T > T_c$, the spin glass correlation length ξ is finite, so for sizes $L \gg \xi$, $P_L(q)$ tends to a Gaussian around $q=0$ of width $\sim N^{-1/2} \sim L^{-d/2}$ so $g \rightarrow 0$. On the other hand, for $T < T_c$, where the infinite system develops a nonzero-order parameter, $g \rightarrow 1$ as $L \rightarrow \infty$. The temperature range about T_c in which g varies between 0 and 1 vanishes as $L \rightarrow \infty$ so g is a step function at T_c in this limit. More precisely, the variation of g is given by the finite size scaling ansatz⁵

$$g_L(T) = \bar{g}(L^{1/\nu}(T - T_c)), \quad (20)$$

where \bar{g} is a scaling function, dependent on L and T only in this combination. Equation (19) assumes that for large enough sizes, L/ξ is the only relevant parameter. It predicts that $g_L(T_c)$ is independent of L so that curves for different L must all cross at T_c , with $g_L(T)$ a decreasing function of L above T_c , and an increasing function of L below T_c . Furthermore, the exponent ν may be extracted from the slopes of the $g_L(T)$ curves at T_c for different L , or by determining the ν for which the data for different L and T are best fit by the scaling form, Eq. (19). This procedure was found⁵ to give good results for the infinite-range Sherrington-Kirkpatrick¹¹ model where T_c and ν

are known exactly.

In addition, at a critical point, the entire overlap distribution $P_L(q)$ is expected to scale according to⁵

$$P_L(q) = L^{\beta/\nu} \bar{P}(qL^{\beta/\nu}) \quad (T = T_c), \quad (21)$$

where β is the order parameter exponent in Eq. (9) and \bar{P} is a scaling function with no dependence on L other than that which enters in implicitly through the argument of \bar{P} . The spin-glass susceptibility χ_{SG} has the finite-scaling form

$$\chi_{\text{SG}} = L^{2-\eta} \bar{\chi}(L^{1/\nu}(T - T_c)), \quad (22)$$

where $\bar{\chi}$ is the scaling function, so that at T_c

$$\chi_{\text{SG}} \sim L^{2-\eta} \quad (T = T_c). \quad (23)$$

Hence the exponent η can be determined either by requiring that all the data for $P_L(q)$ at $T = T_c$ can be collapsed on to the scaling form, Eq. (21), or, more simply, from a log-log plot of χ_{SG} against L for $T = T_c$, using Eq. (23).

III. EQUILIBRATION

It is very important to ensure that the results obtained describe *equilibrium fluctuations*. One problem is that we will always be interested in temperatures below the transition temperature of the pure system, the ‘‘Griffiths¹² phase’’, where the spectrum of relaxation times tends to infinity; there is long time tail in the dynamic correlation functions.¹³ Thus *in principle* one always makes an error in a simulation of the infinite system which is over a finite time. However, the weight in the long time tail is small so that *in practice* the error turns out to be very small and can be less than statistical errors for simulations of only moderate length provided one is some way above the spin glass T_c (but still in the Griffiths phase). Furthermore, the spectrum of relaxation times is always finite in a finite system so one can theoretically run the system for longer than the longest relaxation time and so be truly in equilibrium. In practice, though, one needs a criterion which determines whether any error made in being not quite in equilibrium is acceptably small (for example smaller than the statistical fluctuations). We know of no *rigorous* such criterion but we have found that the following procedure⁵ works well in practice.

For each set of bonds, we simulate two independent set of spins for t_0 steps to equilibrate followed by τ_0 further steps, where $\tau_0 \geq t_0$, to perform the averaging. The question is then whether t_0 is large enough. We have already noted that the overlap distribution can be computed two ways, firstly using time-dependent correlation functions for a single set of spins, Eq. (15), and secondly using two independent sets of spins with the same interactions according to Eq. (17). If t is very small, then $Q(t)$ in Eq. (15) is close to unity, so $P(q)$ from time dependent correlations is strongly peaked near $q = 1$ and the corresponding spin-glass susceptibility will be $\simeq N$, much larger than the equilibrium result. On the other hand, we start our two sets of spins in initially random configurations so that if t is small, $Q'(t) \sim 1/N^{1/2}$, so $P(q)$, derived from Eq. (17) is a Gaussian of width $N^{-1/2}$, and $\chi_{\text{SG}} \simeq 1$.

Hence, if t_0 is smaller than the time to equilibrate within the desired accuracy then χ_{SG} from the two replicas is smaller than the equilibrium value while χ_{SG} from the time-dependent correlation function is too large. We evaluate χ_{SG} (and g_L) these two different ways with $\tau_0=t_0$, and t_0 given successively by the logarithmic sequence 10,30,100,300,1000, . . . , etc. As expected, we find that our two estimates for χ_{SG} approach each other, the replica result increasing monotonically and the result from time-dependent correlations decreasing monotonically. Further, once the two estimates agree for some t_0 they continue to agree for longer times and remain constant aside from statistical fluctuations showing that this is the equilibrium value, see Fig. 1. In Fig. 2 we see that the corresponding two estimates for g_L also approach the equilibrium value from opposite directions.

For each value of T and L we only accepted the results of the run if the two estimates had converged within the errors bars. Otherwise we ran, if possible, for a longer time to try to achieve convergence. If it was not possible to achieve convergence within reasonable computer time, we ignored this value of T and L in the analysis. We emphasize that it is much better to test for equilibrium by requiring that two results agree than by simply looking to see whether one result is time dependent. Since relaxation takes place slowly, roughly logarithmically, results can appear to be independent of time even when equilibrium has not been reached.

The monotonic approach of the two estimates for χ_{SG}

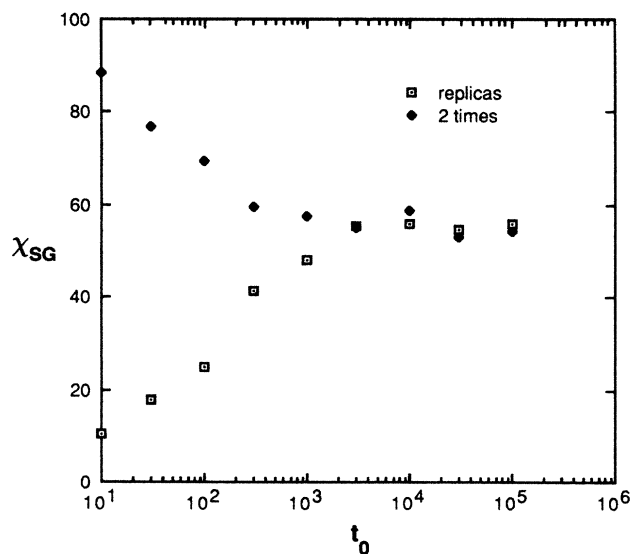


FIG. 1. Plot of χ_{SG} for the four-dimensional model with Gaussian interactions at $T=1.4$ for $L=4$, averaged over 100 sets of bonds. We compute χ_{SG} both from the overlap between two replicas and from spins of one replica at two different times, as described in the text, as a function of equilibration time t_0 . One sees that the replica value increases to the equilibrium value monotonically whereas the “two-time” value decreases monotonically. Once the two estimates agree, they do not change on further increasing t_0 showing that this is the equilibrium value.

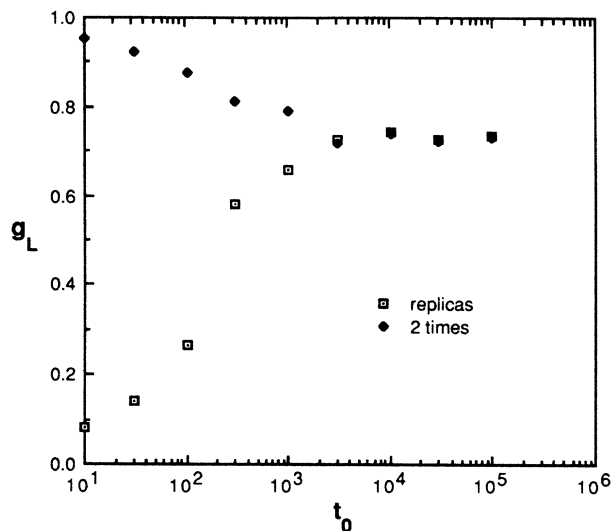


FIG. 2. Same as for Fig. 1, but for g_L .

or g to their equilibrium values from above and below can be physically pictured as the monotonic rise of the equilibrium correlations from the uncorrelated case (infinite temperature) obtained from the randomly initialized replicas, and the monotonic fall of the autocorrelation from the perfectly correlated ($t=0$) limit. For the models, sizes, and temperatures studied, within our statistical fluctuations, the two functions appear to be monotonic, and consequently converge to each other at the equilibrium value. However, it should be borne in mind when applying this procedure, that it is possible in certain more complicated models the behavior may be nonmonotonic and near convergence of the two may not imply that the infinite time limit lies in between the two results. A possible example could be systems with two widely separated length scales. In such a case, establishment of equilibrium over the shorter length scale may give the appearance of near convergence of some time-dependent correlation function which is relatively insensitive to the longer length scale, whereas another quantity which depends primarily on the large length behavior may be far from equilibrium. Keeping such special cases in mind, we feel that the procedure described above is more reliable than others used in the literature, that we are aware of. In particular, we have found it reliable for both short (Figs. 1 and 2) and long⁸ range spin glasses, with no evidence of the pathological scenario discussed above for these systems.

IV. RESULTS IN TWO DIMENSIONS

Our results in $d=2$ are for the $\pm J$ distribution only, which has previously^{7,14-17} been shown to have a zero temperature transition. The behavior of the model with a $\pm J$ distribution differs from that of a continuous distribution because it has a finite ground state entropy per spin. This high degeneracy gives a power law decay of correlations at $T=0$, so $\eta \neq 0$ according to Eq. (6) whereas any continuous distribution has a unique ground state so $\eta=0$. One interesting question is the value of η for the

$\pm J$ model.

Figure 3 shows data for g_L for various lattice sizes averaged over between 64 and 512 bond configurations chosen at random, *independently for each size and temperature*. The point at $T=0$ for $L=4$ is obtained by exact enumeration of all states for a similar number of bond realizations, rather than by Monte Carlo techniques. We see that the data for different sizes come together only when the value of g seems to have saturated to the zero temperature limit [which is different from unity because of the large ground-state degeneracy so $P(q)$ averaged over ground states is not just a single δ function at $g=1$]. This behavior is precisely what is expected at zero temperature transition. A scaling plot of g_L against $L^{1/\nu}T$ is given in Fig. 4 for $1/\nu=0.38$. From Eq. (20), all the data should collapse on to the same curve if $T_c=0$ and ν is chosen correctly. We see that this indeed occurs, though not perfectly, presumably because of systematic corrections to finite size scaling. Choosing different values of ν we estimate

$$\nu=2.6\pm 0.4 (\pm J). \quad (24)$$

which agrees with earlier estimates¹⁵⁻¹⁷ for the $\pm J$ model. Incidentally, the Gaussian distribution seems to have a larger value of ν (Refs. 18-21) indicating that the $\pm J$ model, which has a ground-state entropy, is in a different universality class when $T_c=0$.

Analogous plots for χ_{SG} are given in Figs. 5 and 6, where $\eta=0.2$, $1/\nu=0.38$. Requiring that the low-temperature data scales severely constrain η and we find

$$\eta=0.2\pm 0.05 (\pm J). \quad (25)$$

This is lower than Morgenstern and Binder's¹⁴ result, $\eta=0.4\pm 0.1$ but agrees with McMillan¹⁶ who finds $\eta=0.28\pm 0.04$ and with a recent calculation of Bray and Moore²² who get $\eta=0.20\pm 0.02$. From the scaling law, Eq. (5), the nonlinear susceptibility exponent is found to be

$$\gamma=4.6\pm 0.5 (\pm J). \quad (26)$$

This is somewhat smaller than the high-temperature result of Singh and Chakravarty⁷ who find $\gamma=5.3\pm 0.3$,

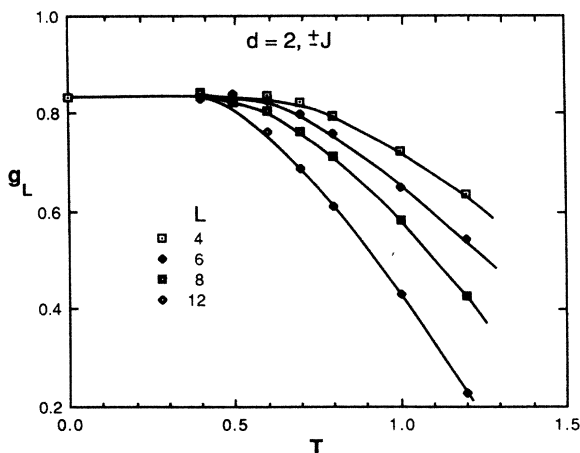


FIG. 3. Plot of g_L against T for various sizes in $d=2$ for the $\pm J$ distribution. The lines are just guides to the eye.

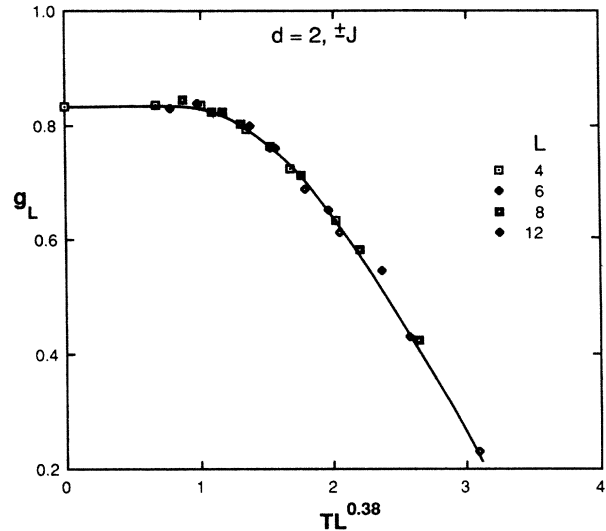


FIG. 4. A fit to the data in Fig. 3 to the finite size scale formula, Eq. (20), with $T_c=0$ and $1/\nu=0.38$ for the $\pm J$ distribution in $d=2$.

though the error bars do overlap. We emphasize that these calculations cannot definitely rule out a very low T_c but, bearing in mind that $T_c^{MF}=2$ and our data certainly rule out a transition with $T_c \gtrsim 0.3$, we concur with earlier work that $T_c=0$ beyond reasonable doubt. We also point out that *the error bars given are estimates that demarcate the region beyond which the data do not scale well, given the statistical errors; they do not allow for systematic errors due to corrections to finite-size scaling*. This is implicit in results in Secs. V and VI as well.

V. RESULTS IN THREE DIMENSIONS

We have carried out simulations on both the $\pm J$ and Gaussian distributions to test whether they have the same critical behavior. Our earlier⁵ results for the $\pm J$ model,

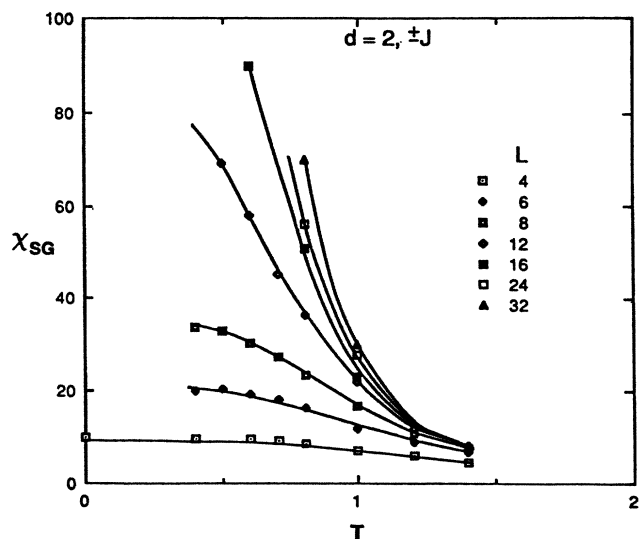


FIG. 5. Plot of χ_{SG} against T in $d=2$ for the $\pm J$ distribution. The lines are just guides to the eye.

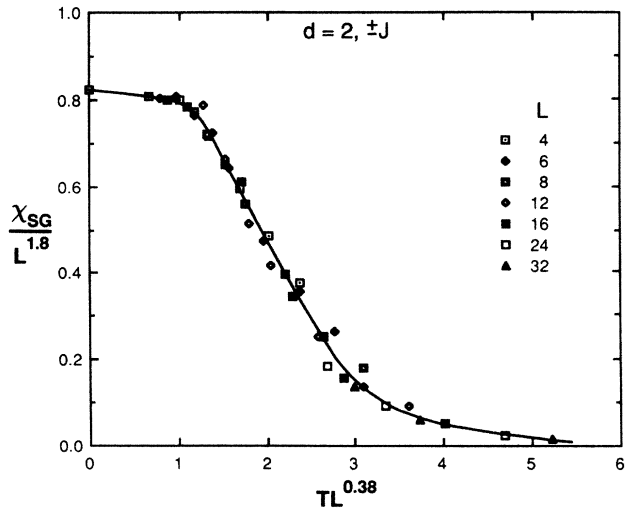


FIG. 6. A fit to the data in Fig. 5 to the finite size scaling formula, Eq. (22), with $T_c=0$, $\eta=0.2$, and $1/\nu=0.38$.

which were averaged over between 100 and 1000 samples, showed evidence for a transition at $T_c \simeq 1.2$, in agreement with other simulations.^{2,3} Recent series expansion results⁷ concur with both the transition temperature and the exponents above T_c . However, the curves of g for different sizes (in Ref. 5) did not splay out below T_c as expected if long-range spin-glass ordering occurs. Rather, they stick together as if all temperatures below T_c were critical. However, Fisher and Huse²³ and Bray and Moore²² argue that the correlation function $G_2(r)$ in Eq. (6) does not decay exponentially with r to its long-distance value, q^2 , below T_c but rather approaches q^2 with a (small) inverse power of r . This means that below T_c the system would seem to be critical up to some characteristic size and only for larger sizes would one see ordering. It is therefore probable that our data below T_c , which was for a small range of sizes $L \leq 8$, was influenced by this strong finite-size effect and that ordering does occur. Recently Ogielski²⁴ has calculated g_L for a larger range of sizes than we could, using the Bell Laboratories special purpose Ising computer. In Fig. 7 we combine his results with ours and see that the expected splaying out below T_c still does not occur. If indeed the low-temperature phase has long-range order, we expect that it would do so for larger sizes, but envisage little possibility of demonstrating this directly by Monte Carlo simulations because the equilibration time rises very rapidly with size. A scaling plot is shown in Fig. 8, using $T_c=1.2$, $\nu=1.3$, consistent with our earlier values of $T_c=1.2^{+0.1}_{-0.2}$, and

$$\nu=1.3 \pm 0.3 \quad (\pm J), \quad (27a)$$

$$\eta=-0.3 \pm 0.2 \quad (\pm J). \quad (27b)$$

Note that the data seems to scale well above T_c but not below it, presumably due to the finite-size corrections discussed above. Thus adding data for g_L from larger sizes does not significantly change our estimates for T_c or ν but neither does it resolve the problem of lack of scaling

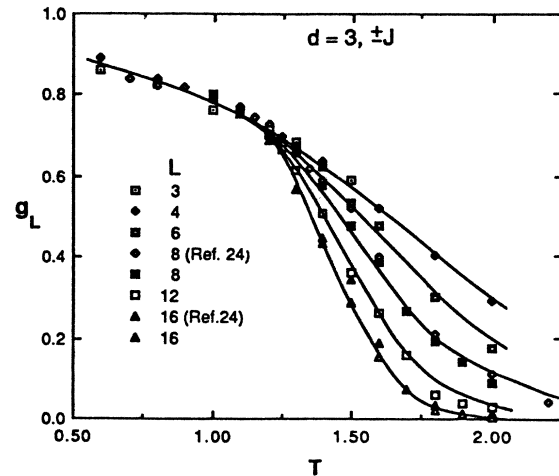


FIG. 7. Plot of g_L against T in $d=3$ for the $\pm J$ distribution. The lines are just guides to the eye.

below T_c .

Of course, one could always argue that the data is consistent with T_c somewhat lower than 1.2 and that the critical region is very narrow. However, one then has to understand why the same estimate is obtained from large (essentially infinite) size systems^{2,3} and high-temperature series expansions.⁷

Attempting to make the $g_L(T)$ data scale with $T_c=0$ does not work with any value of ν . The “best fits,” obtained with very large values of ν , show systematic deviations from the scaling form as shown in Fig. 9 with $1/\nu=0.13$. One may argue again that the scaling region has not been reached. However, our results for $d=2$, which beyond reasonable doubt, has $T_c=0$, do seem to scale in the same region of T/T_c^{MF} .

There are other differences between our $d=2$ and our $d=3$ results. For one, our $g_L(T)$ curves in $d=2$ do not quite meet down to the lowest temperatures where we

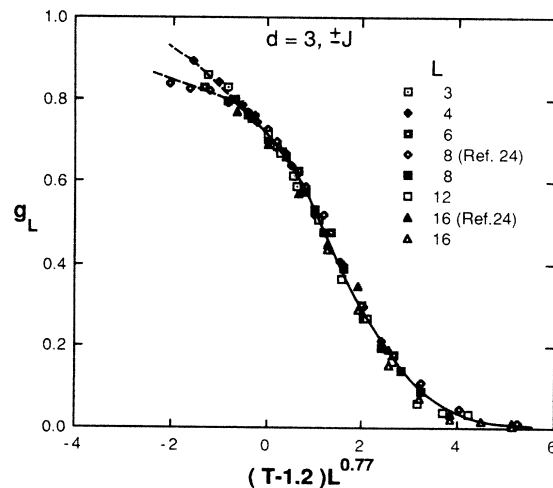


FIG. 8. Scaling plot of the data in Fig. 7, fitted to Eq. (20), with $T_c=1.2$, and $1/\nu=0.77$.

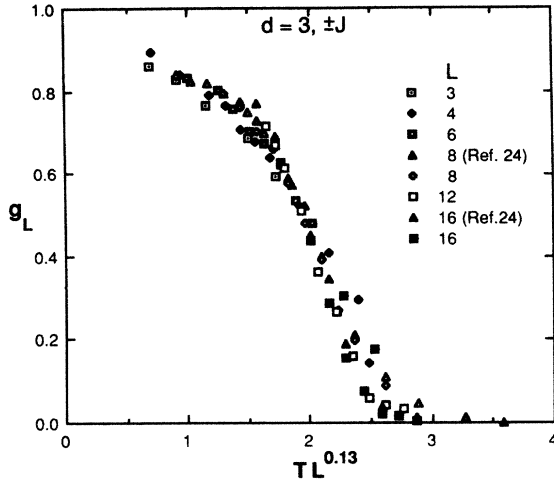


FIG. 9. Attempted scaling plot of the data in Fig. 7 according to Eq. (20), with $T_c = 0$ and "best fit" value of $1/\nu = 0.13$.

could equilibrate ($T=0.4$) which is 20% of T_c^{MF} . By contrast, in $d=3$, the height T data seem headed to cross at an actual T_c of about 50% of T_c^{MF} . Furthermore, in $d=2$, as the curves of $g_L(T)$ for different sizes approach each other, their T dependences also diminishes, so the L dependence and T dependence go hand in hand. This does not appear to be so at low T in $3d$. The $T=0$ limit of g_L appears to be less than unity in $d=2$, consistent with a model which has $T_c=0$ and degenerate ground states (finite $T=0$ entropy), whereas the data for the $\pm J$ model in $d=3$ are consistent with $g=1$ at $T=0$.

It may be argued that some of the unusual behavior seen in the $\pm J$ model below T_c is because this distribution is far from the fixed-point distribution. For this reason, and also to check whether the $\pm J$ model is in the same universality class as a model with a continuous distribution when T_c is finite, we have made a similar study for the case of Gaussian bonds. Results for $g_L(T)$ are shown in Fig. 10, each point represents an average 500–2000 samples chosen *independently for each L and T*. Without the use of special purpose computers and because of the somewhat lower T_c we were limited to sizes with linear dimension $L \leq 6$. For these sizes, the results look rather similar to the $\pm J$ model. The $g_L(T)$ data come together at a critical temperature $T_c \sim 0.9-1.0$ and are found to scale well with

$$\nu = 1.6 \pm 0.4 \quad (\text{Gaussian}), \quad (28)$$

see Fig. 11, depending upon the T_c chosen (lower ν for higher T_c). These results are in good agreement with the results of McMillan²⁵ on the same model ($T_c = 1.0 \pm 0.2, \nu = 1.8 \pm 0.5$) but Bray and Moore²⁶ obtain a considerably larger ν , namely, $\nu = 3.3 \pm 0.6$. This discrepancy remains unexplained. Again, the data below T_c do not fan out as expected, despite the relatively strong variation with T (more than the $\pm J$ model).

To obtain the exponent η we have also calculated χ_{SG} and show a scaling plot for $\eta = -0.45, \nu = 1.25$ in Fig. 12. Note that χ_{SG} scales better with a rather smaller value of ν than used for g_L in Figure 11. This possibly

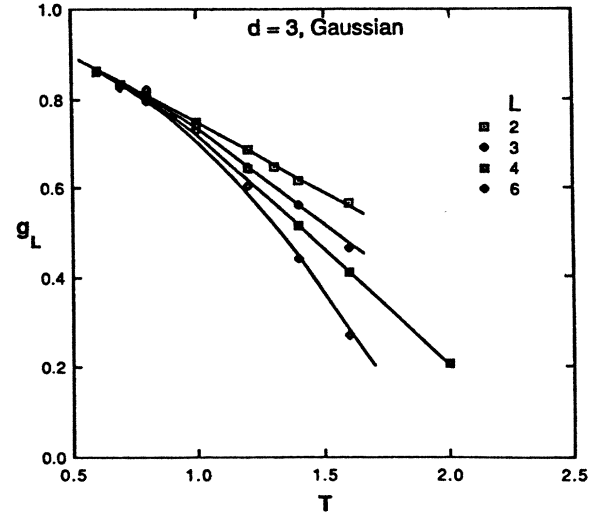


FIG. 10. Plot of g_L against T in $d=3$ for the Gaussian distribution. The lines are just guides to the eye.

reflects corrections to scaling and the difference may be a measure of uncertainty in the exponent. It is reassuring that the (presumably) more accurate value obtained from the much more extensive work on the $\pm J$ model is spanned by the two estimates of ν in the Gaussian case. Notice also that the $L=2$ points do not scale well, indicating that this size is too small. Our overall estimate for η is

$$\eta = -0.4 \pm 0.2 \quad (\text{Gaussian}), \quad (29)$$

which is consistent with our values for the $\pm J$ model in Eq. (27).

Our data for $d=3$ are therefore consistent with the $\pm J$ and Gaussian distributions being in the same universality

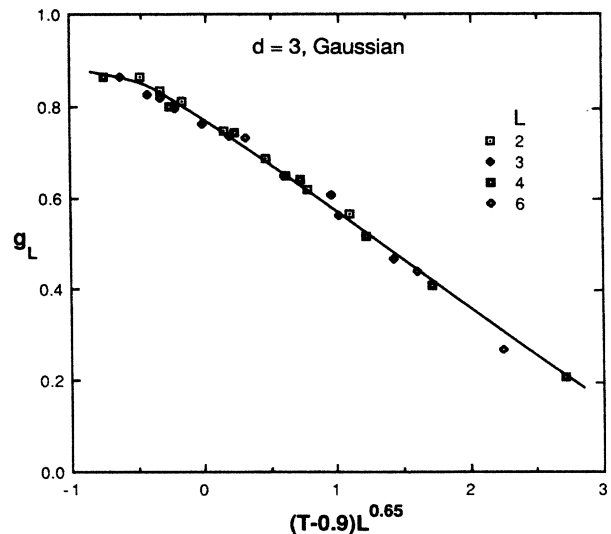


FIG. 11. Scaling plot of the data in Fig. 10, fitted to Eq. (20), with $T_c = 0/9$, and $1/\nu = 0.65$.

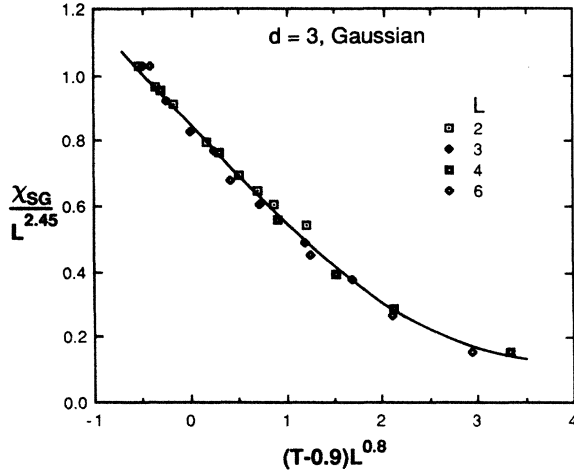


FIG. 12. Scaling plot of χ_{SG} for the Gaussian distribution in $d=3$ fitted to Eq. (22), with $T_c=0.9$, $\eta=-0.45$ and $1/\nu=0.8$.

class at the finite T_c , though the error bars are somewhat large, particularly for the Gaussian case.

VI. RESULTS IN FOUR DIMENSIONS

In order to clarify whether the apparently marginal behavior we find for $T < T_c$ in $d=3$ is generic to the low-temperature phase of short-range spin glasses or is special to three dimensions, we have performed simulations for a Gaussian bond model in four dimensions. Our results for $g_L(T)$ for $2 \leq L \leq 6$ are shown in Fig. 13 where each point is an average of 200–800 samples. The curves indicate $T_c=1.75 \pm 0.05$ and they *do* fan out below T_c showing that long-range spin-glass order occurs below the transition. Note that the mean-field estimate for the transition temperature is $T_c^{MF} = \sqrt{8} = 2.83$. Except for $L=2$ the data scales both below as well as above T_c as shown in Fig. 14 where we have used a correlation-length exponent

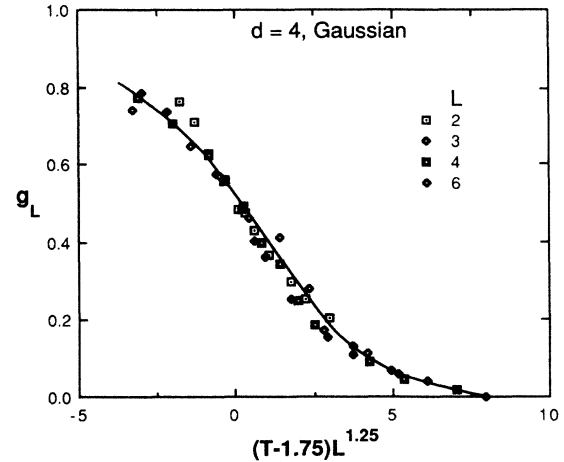


FIG. 14. Scaling plot of the data in Fig. 13, fitted to Eq. (20), with $T_c=1.75$ and $1/\nu=1.25$.

$\nu=0.8$. In three dimensions too, $L=2$ did not scale well; we suspect this is perhaps because periodic boundary conditions cause double connections for this size, and only this size. We estimate the range of ν allowed by our data to be

$$\nu=0.8 \pm 0.15 \quad (\text{Gaussian}) . \quad (30a)$$

Data for χ_{SG} are plotted in Fig. 15 while the scaling plot is shown in Fig. 16. These imply

$$\eta=-0.3 \pm 0.15 \quad (\text{Gaussian}) , \quad (30b)$$

which combined with Eqs. (30a) and (5) gives

$$\gamma=1.8 \pm 0.4 \quad (\text{Gaussian}) . \quad (30c)$$

The above value for γ agrees well with a recent estimate of $\gamma=2.0 \pm 0.4$ obtained for a $\pm J$ distribution from high series expansions.⁷ Although the error bars are large, the

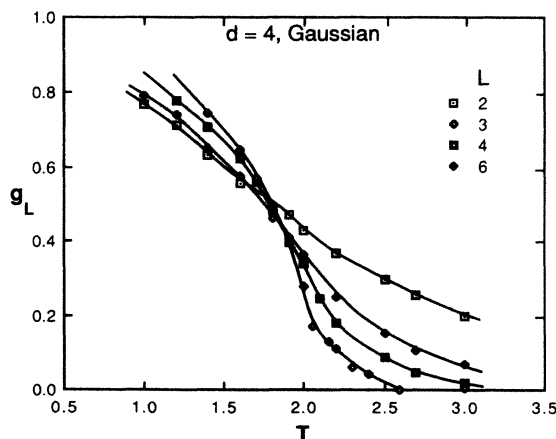


FIG. 13. Results for g_L against T in $d=4$ for the Gaussian distribution. T_c is estimated to be 1.75 ± 0.05 from the intersection of the curves. The curves for different sizes play out below T_c showing that the spin glass order parameter is nonzero. The lines are just guides to the eye.

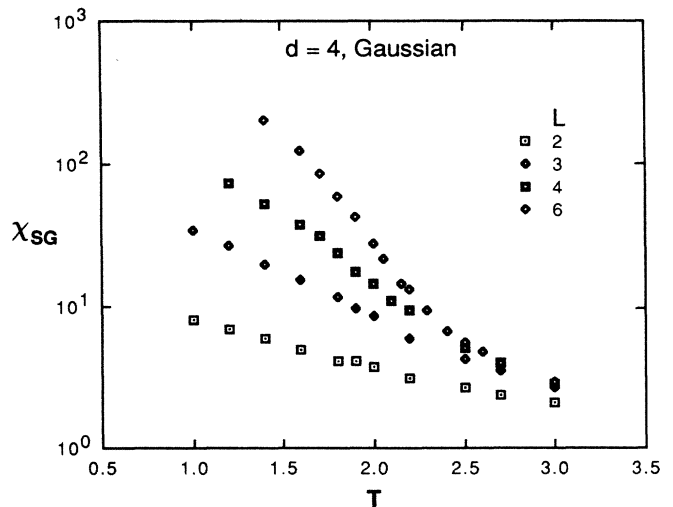


FIG. 15. Data for χ_{SG} in $d=4$ for a Gaussian distribution. Note the logarithmic scale.

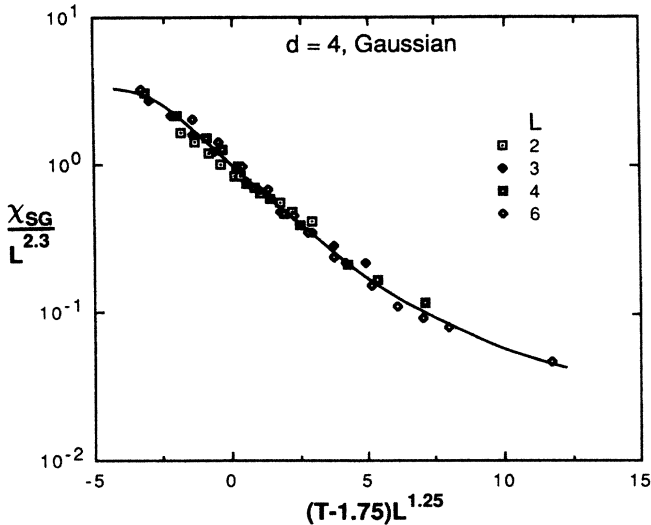


FIG. 16. Scaling plot of the data in Fig. 15, fitted to Eq. (22), with $T_c = 1.75$, $\eta = -0.3$, and $1/\nu = 1.25$.

results are consistent with the $\pm J$ and Gaussian distributions lying in the same universality class.

VII. CONCLUSIONS

We have carried out a fairly comprehensive study of Ising spin glasses on hypercubic lattices with nearest-neighbor interactions in two, three, and four dimensions. Using finite-size scaling of data obtained via Monte Carlo simulations on a wide range of lattice sizes, we find that

in $d=2$, where the transition is at $T_c=0$, the $\pm J$ and Gaussian distributions have different critical behavior. However in the higher dimensions, $d=3$ and 4 , where T_c is nonzero, they appear to be in the same universality class. Our finite-size scaling results show that conventional long-range ordering takes place below T_c in $d=4$. This may also be true in $d=3$, though a simple finite-size-scaling analysis of our data remains at variance with this result. A plausible explanation is the existence of large corrections to finite-size scaling in $d=3$ owing to the proximity of the lower critical dimension of short-range Ising spin glasses.

ACKNOWLEDGMENTS

We would like to thank A. J. Bray, D. S. Fisher, D. A. Huse, M. A. Moore, M. Nauenberg, A. T. Ogielski, D. Sherrington, and J. D. Reger for helpful discussions. We would also like to thank A. T. Ogielski for permission to reproduce his unpublished results in Figs. 7 and 8. Most of the work on the $\pm J$ distribution was done on the Distributed Array Processor at Queen Mary College, London, which was supported by the Science and Engineering Research Council of the United Kingdom. The work of one of us (A.P.Y.) was supported by the National Science Foundation, under Grants No. DMR-84-19536 and No. DMR-85-10593. We are also grateful for the hospitality of the Institute for Theoretical Physics at Santa Barbara, where this work was supported by the National Science Foundation through Grant No. PHY-82-17853, supplemented by funds from the U.S. National Aeronautics and Space Administration.

¹For a recent review of numerical simulations, see R. N. Bhatt and A. P. Young, in *Heidelberg Colloquium on Glassy Dynamics*, edited by J. L. van Hemmen and I. Morgenstern (Springer, Berlin, 1987), p. 215. For a more general review of spin glasses, see K. Binder and A. P. Young, *Rev. Mod. Phys.* **58**, 801 (1986).
²A. T. Ogielski and I. Morgenstern, *Phys. Rev. Lett.* **54**, 928 (1985); *J. Appl. Phys.* **57**, 3382 (1985); A. T. Ogielski, in *Heidelberg Colloquium on Glassy Dynamics*, edited by J. L. van Hemmen and I. Morgenstern (Springer, Berlin, 1987), p. 190.
³A. T. Ogielski, *Phys. Rev. B* **32**, 7384 (1985).
⁴A. P. Young, *J. Phys. C* **18**, L517 (1984).
⁵R. N. Bhatt and A. P. Young, *Phys. Rev. Lett.* **54**, 924 (1985).
⁶See, e.g., M. N. Barber, in *Phase Transitions and Critical Phenomena*, edited by C. Domb and J. Lebowitz, (Academic, New York, 1983), Vol. 8, p. 146.
⁷R. R. P. Singh and S. Chakravarty, *Phys. Rev. Lett.* **57**, 245 (1986).
⁸R. N. Bhatt and A. P. Young, *J. Magn. Mag. Mater.* **54-57**, 191 (1986).
⁹S. R. Edwards and P. W. Anderson, *J. Phys. F* **5**, 965 (1975).
¹⁰K. Binder, *Z. Phys. B* **48**, 319 (1982).

¹¹D. Sherrington and S. Kirkpatrick, *Phys. Rev. Lett.* **35**, 1792 (1975).
¹²R. B. Griffiths, *Phys. Rev. Lett.* **23**, 17 (1969).
¹³M. Randeria, J. P. Sethna, and R. G. Palmer, *Phys. Rev. Lett.* **54**, 1321 (1985).
¹⁴I. Morgenstern and K. Binder, *Phys. Rev. Lett.* **43**, 1615 (1979); *Phys. Rev. B* **22**, 288.
¹⁵A. P. Young, *J. Phys. C* **17**, L517 (1984).
¹⁶W. L. McMillan, *Phys. Rev. B* **28**, 5216 (1983).
¹⁷H. F. Cheung and W. L. McMillan, *J. Phys. C* **16**, 7027 (1983).
¹⁸W. L. McMillan, *Phys. Rev. B* **29**, 4026 (1984); **30**, 476 (1984).
¹⁹A. J. Bray and M. A. Moore, *J. Phys. C* **17**, L463 (1984).
²⁰H. F. Cheung and W. L. McMillan, *J. Phys. C* **16**, 7033 (1983).
²¹D. A. Huse and I. Morgenstern, *Phys. Rev. B* **32**, 3032 (1985).
²²A. J. Bray and M. A. Moore, in *Heidelberg Colloquium on Glassy Dynamics*, edited by J. L. van Hemmen and I. Morgenstern (Springer, Berlin, 1987), p. 121.
²³D. S. Fisher and D. A. Huse, *Phys. Rev. Lett.* **56**, 1601 (1986).
²⁴A. T. Ogielski (private communication) Ogielski used the same samples for all T , unlike our simulations.
²⁵W. L. McMillan, *Phys. Rev. B* **31**, 340 (1985).
²⁶A. J. Bray and M. A. Moore, *Phys. Rev. B* **31**, 631 (1985).